Appl. Phys. B 65, 351–355 (1997)

Applied Physics B Lasers and Optics

Measurement of the phase anisotropy of very high reflectivity interferential mirrors

F. Brandi[1,2], F. Della Valle[3], A.M. De Riva[4], P. Micossi[3], F. Perrone[2,5], C. Rizzo[1,*], G. Ruoso[1], G. Zavattini[4]

[1] Laboratori INFN, via Romea 4, 35020 Legnaro (PD), Italy
(Fax: +39-49/641925, E-mail: rizzo@legnaro.infn.it)
[2] Dipartimento di Fisica, Piazza Torricelli 1, 56100 Pisa, Italy
(Fax: +39-50/48277)
[3] Dipartimento di Fisica and INFN, via Valerio 2, 34127 Trieste, Italy
(Fax: +39-40/6763350)
[4] Dipartimento di Fisica and INFN, via Paradiso 12, 44100 Ferrara, Italy
(Fax: +39-532/762057)
[5] INFN, via Livornese 582/a, 56010 S. Piero a Grado (PI), Italy

Received: 28 January 1997

Abstract. We have measured the phase anisotropy of four very high reflectivity ($R > 0.999969$) interferential mirrors for polarized light at strictly normal incidence by studying the birefringence properties of a Fabry–Pérot cavity to which a Nd:YAG laser has been frequency locked. We found phase anisotropies per reflection ranging from less than 2×10^{-7} rad to 2×10^{-6} rad.

PACS: 42.70; 42.80

Recently high-finesse Fabry–Pérot cavities [1] have found applications in several advanced fields; for instance gravitational wave detection with interferometers [2, 3], optical sensors for gravitational wave bar antennas [4], metrology [5], gyrometry [6], and parity violation experiments [7]. In particular their use has been proposed to increase the sensitivity of ellipsometer apparata designed to measure the vacuum magnetic birefringence [8–10] and gas magnetic birefringence [11].

In general, when a linearly polarized light beam is reflected by an interferential mirror, the reflected light acquires a slight elliptical polarization. This fact is a source of noise and systematic errors in all of the above-mentioned experiments. In [12], for example, the authors discuss this noise problem for an apparatus such as the one proposed in [10].

Experimental studies of the birefringence properties of interferential mirrors have been conducted [13–17]. The results show that birefringence for normal-incidence reflection could be as large as 3×10^{-4} for a 0.9983 reflectivity mirror [15]. The value of birefringence and the direction of the birefringence axis were also shown to vary for different reflection points on the mirror surface [15].

In [18], the authors proved that in a Fabry–Pérot cavity at resonance the changes in the light polarization caused by the phase anisotropy of the mirror surface add coherently. Moreover, since in the case of a Fabry–Pérot the incidence on the mirror is strictly normal, the birefringence due to the off-normal incidence vanishes. The finesse F of the Fabry–Pérot cavity [18] was about 7000 ($R \approx 0.99955$), the measured phase anisotropy per reflection was of the order of 10^{-6} rad.

A phase anisotropy per reflection of the same order of magnitude has been also reported in [17]. The mirror was part of a Fabry–Pérot cavity of finesse around 100 000 ($R \approx 0.999969$). A higher phase anisotropy of the order of 10^{-3} rad is reported in [9] for mirrors of a Fabry–Pérot cavity with finesse 300 ($R \approx 0.9895$).

In this letter we report the measurements of the phase anisotropy of two pairs of interferential mirrors used to realize a Fabry–Pérot cavity to which a Nd:YAG laser was frequency locked by means of the Pound–Drever technique [19]. The mirrors are high-reflectivity spherical mirrors (reflectivity $R > 0.999969$, radius of curvature $R_c = 11$ m, BK7 substrate) and they were supplied by Research Electro-Optics (Boulder, Colorado).

The measured phase anisotropy per reflection ranges from less than 2×10^{-7} rad to 2.4×10^{-6} rad.

In Fig. 1a simplified scheme of the apparatus is shown. The measurements reported in this article were performed during the tests of the PVLAS (Polarizzazione del Vuoto con LASer) experiment [8]. PVLAS has been designed to meas-

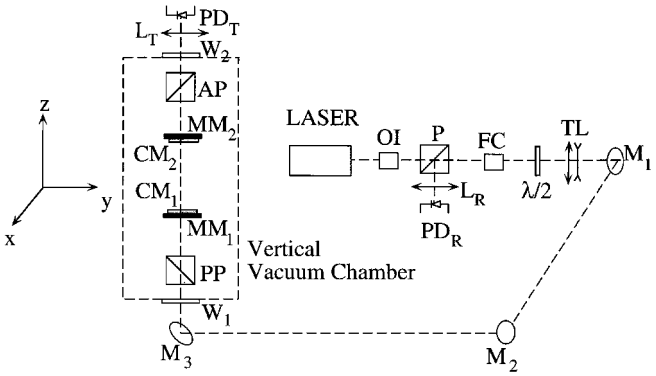

Fig. 1. Simplified scheme of the apparatus. OI optical isolator; P, PP, AP polarizer prisms; L_R, L_T lenses; PD_R, PD_T photodiodes; FC Faraday cell; $\lambda/2$ half-wave plate; TL telescope; M_1, M_2, M_3 steering mirrors; W_1, W_2 windows; MM_1, MM_2 tilting stages; CM_1, CM_2 cavity mirrors; coordinate axis are also shown

Permanent address: INFN, Via Valerio 2, 34127 Trieste, Italy

ure the vacuum magnetic birefringence by using a very sensitive ellipsometer that will be based on a vertical 6-m-long very high finesse Fabry–Pérot cavity. The servo system used to lock the laser to the high-finesse Fabry–Pérot cavity has already been discussed [20].

The light source is a tunable NPRO laser emitting about 15 mW of power at a wavelength of $\lambda = 1.064\,\mu\text{m}$ ($\nu = 2.82 \times 10^{14}$ Hz). The laser light after crossing a two-stage optical isolator, OI, enters the polarizing cube beam splitter P which is set for maximum transmission. The Faraday cell FC rotates the polarization by a 45° angle and a half-wave plate $\lambda/2$ is used to change the polarization direction of the beam. A telescope TL is used to match the laser beam to the cavity FP. Mirrors M_1 and M_2 are mounted on tilting stages and are used to allow the alignment of the beam with the optical axis of the cavity. When the cavity and the beam are properly aligned light coming back from the cavity follows the same optical path as incoming light. After it crosses the Faraday cell, FC, the polarization angle of the reflected light is rotated a further 45° so that the reflected light can be extracted from the main path as the ordinary ray of polarizer prism P. Mirror M_3 steers the beam in the vertical direction. The polarizer prism PP is used to linearly polarize the laser beam before it enters the FP made of the two mirrors CM_1 and CM_2. The polarizer prism AP is then used to analyze the polarization state of the light transmitted by the cavity. The cavity mirrors CM_1 and CM_2 and the polarizer prisms PP and AP are contained in a vacuum chamber and mounted on stages designed to rotate the optical elements around the z axis (see Fig. 1), to tilt them around x and y axis, and to translate along x and y axis. Appropriate manual feedthrough for vacuum allowed us to precisely align the optical elements from outside the vertical vacuum chamber. The photodiode PD_R collects the reflected light, focused by the lens L_R, giving the main signal for the Pound–Drever locking scheme. The photodiode PD_T, on the other hand, collects the light transmitted by the cavity and analyzed by the polarizer prism AP. The lens L_T focuses the transmitted light onto this photodiode. Two windows (W_1 and W_2) allow the light to enter and exit the vacuum chamber. The length of the Fabry–Pérot cavity is 2.15 m.

The principle of the experiment is shown in Fig. 2. A light beam propagating along the z direction is linearly polarized at an angle θ_P with respect to the x axis. The phase anisotropies of the coatings of the cavity mirrors CM_1 and CM_2 are schematized as two ideal waveplates WP_1 and WP_2 between two isotropic cavity mirrors M_1 and M_2 of reflectivity R. WP_1 has its fast axis along the x axis and a phase anisotropy δ_1. WP_2 has its fast axis at an angle θ_{WP} with respect to the x axis (i.e. with respect to the fast axis of WP_1) and a phase anisotropy δ_2. Thus the phase anisotropy per reflection corresponds to twice the phase anisotropy of the ideal waveplates WP_1 or WP_2.

Light coming from the cavity is analyzed by a polarizer prism crossed with the initial laser polarization. When the laser is frequency locked to the cavity, rotation of the AP polarizer varies the transmitted light from a minimum value I_{EXT} to a maximum value I_T. Therefore, the ellipticity Ψ can be measured as the square root of I_{EXT}/I_T, i.e.

$$\Psi = \sqrt{\frac{I_{EXT}}{I_T}} = f(\theta_P, \theta_{WP}, \delta_1, \delta_2)\,. \tag{1}$$

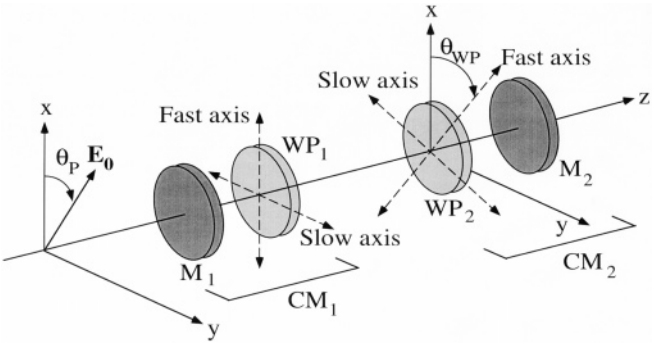

Fig. 2. Principle of the experiment; $\boldsymbol{E}_0$ light polarization vector; CM_1, CM_2 cavity mirrors; M_1, M_2 isotropic mirrors; WP_1, WP_2 waveplates equivalent to the coating of cavity mirrors

To calculate the expression for Ψ as a function of the experimental parameters θ_P, θ_{WP}, δ_1, δ_2 we use the Jones matrix formalism [21]. The following matrices represent the waveplates WP_1 and WP_2

$$\mathbf{WP}_1 = \begin{pmatrix} e^{+i\delta_1/2} & 0 \\ 0 & e^{-i\delta_1/2} \end{pmatrix} \tag{2}$$

$$\mathbf{WP}_2 = \begin{pmatrix} e^{+i\delta_2/2}\cos^2\theta_{WP} + e^{-i\delta_2/2}\sin^2\theta_{WP} & -2i\sin(\delta_2/2)\cos\theta_{WP}\sin\theta_{WP} \\ -2i\sin(\delta_2/2)\cos\theta_{WP}\sin\theta_{WP} & e^{-i\delta_2/2}\cos^2\theta_{WP} + e^{+i\delta_2/2}\sin^2\theta_{WP} \end{pmatrix} \tag{3}$$

The combined effect of the waveplates WP_1 and WP_2 corresponds to the effect of a single equivalent waveplate WP_{EQ} of phase anisotropy δ_{EQ} and with the fast axis at an angle θ_{EQ} with respect to the x axis. Writing then

$$\mathbf{WP}_{EQ} = \begin{pmatrix} e^{+i\delta_{EQ}/2}\cos^2\theta_{EQ} + e^{-i\delta_{EQ}/2}\sin^2\theta_{EQ} & -2i\sin(\delta_{EQ}/2)\cos\theta_{EQ}\sin\theta_{EQ} \\ -2i\sin(\delta_{EQ}/2)\cos\theta_{EQ}\sin\theta_{EQ} & e^{-i\delta_{EQ}/2}\cos^2\theta_{EQ} + e^{+i\delta_{EQ}/2}\sin^2\theta_{EQ} \end{pmatrix} \tag{4}$$

and imposing

$$\mathbf{WP}_{EQ} = \mathbf{WP}_2 \cdot \mathbf{WP}_1 \tag{5}$$

with matrix algebra, and for $\delta_1, \delta_2 \ll 1$ one obtains

$$\delta_{EQ} = \sqrt{(\delta_1 - \delta_2)^2 + 4\delta_1\delta_2\cos^2\theta_{WP}} \tag{6}$$

$$\cos 2\theta_{EQ} = \frac{\delta_1/\delta_2 + \cos 2\theta_{WP}}{\sqrt{(\delta_1/\delta_2 - 1)^2 + 4(\delta_1/\delta_2)\cos^2\theta_{WP}}}\,. \tag{7}$$

When $\delta_1 \gg \delta_2$ (or $\delta_2 \gg \delta_1$), δ_{EQ} does not depend on θ_{WP} and is equal to δ_1 (or δ_2).

In Fig. 3 we show θ_{EQ} for some characteristic values of δ_1 and δ_2. One can see that if $\delta_1/\delta_2 = 1$, θ_{EQ} is equal to $\theta_{WP}/2$; if

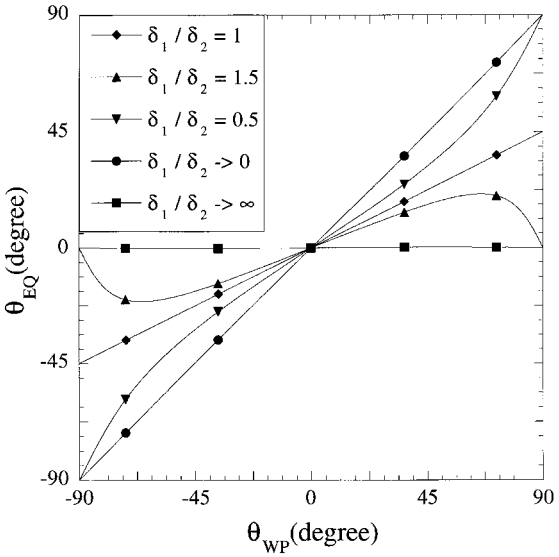

Fig. 3. Plot of the theoretical expressions of $\theta_{\mathrm{EQ}}(\theta_{\mathrm{WP}})$ for some characteristic value of the ratio δ_1/δ_2

$\delta_1/\delta_2 \to \infty$, θ_{EQ} is equal to 0 and finally if $\delta_1/\delta_2 \to 0$, θ_{EQ} is equal to θ_{WP}. Intermediate cases ($\delta_1/\delta_2 = 0.5,\ \delta_1/\delta_2 = 1.5$) are also shown.

To explicitate (1) we calculate the Jones matrix $\mathbf{FP}_{\mathrm{WP}}$ corresponding to a Fabry–Pérot cavity at resonance, taking into account the presence of the waveplate $\mathrm{WP}_{\mathrm{EQ}}$ between the two mirrors. For the sake of simplicity we use the coordinate system in which $\mathbf{WP}_{\mathrm{EQ}}$ is diagonal. For two identical mirrors $\mathbf{FP}_{\mathrm{WP}}$ can therefore be written as

$$\mathbf{FP}_{\mathrm{WP}} = \sum_{n=0}^{+\infty} \left\{ T \left[R \begin{pmatrix} \mathrm{e}^{\mathrm{i}\delta_{\mathrm{EQ}}} & 0 \\ 0 & \mathrm{e}^{-\mathrm{i}\delta_{\mathrm{EQ}}} \end{pmatrix} \right]^n \begin{pmatrix} \mathrm{e}^{\mathrm{i}\delta_{\mathrm{EQ}}/2} & 0 \\ 0 & \mathrm{e}^{-\mathrm{i}\delta_{\mathrm{EQ}}/2} \end{pmatrix} \right\} , \tag{8}$$

where T and R are the mirror transmittivity and reflectivity, respectively. Again, matrix algebra gives as result that

$$\mathbf{FP}_{\mathrm{WP}} = \frac{T}{1-R} \begin{pmatrix} \exp\left[\mathrm{i} \left(\frac{1+R}{1-R} \right) \frac{\delta_{\mathrm{EQ}}}{2} \right] & 0 \\ 0 & \exp\left[-\mathrm{i} \left(\frac{1+R}{1-R} \right) \frac{\delta_{\mathrm{EQ}}}{2} \right] \end{pmatrix} . \tag{9}$$

$\mathbf{FP}_{\mathrm{WP}}$ corresponds to, apart from the usual Fabry–Pérot transmission factor $T/(1-R)$ [1], to a waveplate of anisotropy $(1+R)/(1-R)\delta_{\mathrm{EQ}}$, i.e. using a Fabry–Pérot cavity one amplifies the effect δ_{EQ} of the original waveplate by a factor $A = (1+R)/(1-R)$. If $R \approx 1$, A can be written as $2F/\pi$, where F is the finesse of the cavity [1].

As we have demonstrated the combination of the two waveplates $\mathbf{WP}_1$ and $\mathbf{WP}_2$ and the Fabry–Pérot cavity at resonance acts on the light polarization as a waveplate $\mathbf{FP}_{\mathrm{WP}}$ of phase anisotropy $\delta = (2F/\pi)\delta_{\mathrm{EQ}}$ with the fast axis at an angle θ_{EQ}. The square of the ellipticity Ψ^2 can be written as

$$\begin{aligned} \Psi^2 &= \frac{I_{\mathrm{EXT}}}{I_{\mathrm{T}}} \\ &= \left(\frac{1-R}{T} \right)^2 \left| \mathbf{AP} \cdot \mathbf{R}(\theta_{\mathrm{EQ}} - \theta_{\mathrm{P}}) \cdot \mathbf{FP}_{\mathrm{WP}} \cdot \mathbf{R}(\theta_{\mathrm{P}} - \theta_{\mathrm{EQ}}) \cdot \begin{pmatrix} 1 \\ 0 \end{pmatrix} \right|^2 \\ &= \frac{\delta^2}{4} \sin^2 2(\theta_{\mathrm{P}} - \theta_{\mathrm{EQ}}) , \end{aligned} \tag{10}$$

where $\mathbf{R}(\alpha)$ is the rotation matrix of an angle α and $\mathbf{AP}$ is the matrix corresponding to the analyzer prism AP set to maximum extinction. We are interested in the phase anisotropy of the two mirrors, i.e. δ_1 and δ_2 in our schema. To recover these two values, we measured Ψ^2 as a function of θ_{P} for different values of θ_{WP}. From the analysis of the experimental values of $\Psi^2(\theta_{\mathrm{P}}, \theta_{\mathrm{WP}})$ one obtains the experimental values of the functions $\delta_{\mathrm{EQ}}(\delta_1, \delta_2, \theta_{\mathrm{WP}})$ and $\theta_{\mathrm{EQ}}(\delta_1/\delta_2, \theta_{\mathrm{WP}})$ and finally from the comparison with the theoretical curves one can evaluate δ_1 and δ_2.

We have tested two pairs of very high reflectivity mirrors, in the following labeled with Roman numerals I and II, respectively. To obtain a good resonance condition of the Fabry–Pérot cavity we have to properly align the laser beam and the geometrical axis of the mechanical supports. Using mirrors M_1 and M_2 we aligned the laser beam to pass through the cavity-mirror tilting stages so that light could hit the center of the mirror itself. The two mirror centers define the cavity axis. The cavity mirror CM_2 was then cleansed with pure ethanol and put in its tilting stage MM_2. Stage MM_2 was then used to send the reflected beam exactly on the same path as the incoming beam. The same procedure was followed for the second mirror CM_1. Since the cavity is vertical, the mirror can be just placed on the tilting stage, thus minimizing the mechanical stresses on the mirror itself, which can produce birefringence [1]. The vacuum chamber was then closed and evacuated. During data taking the pumps were switched off and the pressure inside the vessel was less than 0.1 mbar.

The frequency of the laser was then driven by a triangular wave signal. An infrared-sensitive camera was put before the photodiode PD_{T}. While the laser frequency was swept by the triangular wave the frequency modes of the cavity could be clearly seen on a TV monitor. By slightly adjusting stages MM_1, MM_2, M_1, and M_2, the cavity could be fine tuned on the mode TEM_{00}. The servo system was then turned on and we checked that the laser was locked to the TEM_{00} mode of the cavity. Finally, we removed the camera and again using stages M_1 and M_2 we maximized the intensity transmitted by the cavity at resonance, looking at the signal from the photodiode PD_{T}. To measure the cavity finesse F we measured the cavity decay time, observing the exponential decay of the light coming onto photodiode PD_{T} after the laser was switched to the standby mode [20]. For mirror pair I we obtained a finesse of about 65 000 and for mirror pair II we obtained a finesse of about 110 000. The finesse expected from the data provided by the mirror manufacturer should be at least 100 000. The slightly smaller value measured for mirror pair I is probably due to a defective mirror-cleaning procedure. The relative error of the finesse measurement has been evaluated, by measuring several times the finesse of the cavity during data taking, to be about 10%.

Once the Fabry–Pérot cavity was set up, phase anisotropy measurements could be started. The intensities I_{EXT} and I_T have been measured for different θ_P. To change θ_P we rotated the half-wave plate $\lambda/2$ and consequently the polarizing prism PP. We then rotated the cavity mirror CM_2 around the z axis to perform another measurement of I_{EXT} and I_T as function of θ_P for a different θ_{WP}. The angles θ_{WP} and θ_P were measured relative to the initial angular values θ^0_{WP} and θ^0_P. The absolute value of θ^0_{WP} and θ^0_P were then determined by comparison of the experimental and theoretical curves.

In principle, if the optical axis of the cavity corresponded exactly to the z axis, rotating CM_2 should not affect the alignment of the cavity. In practice we have to slightly realign the cavity for every different θ_{WP}. This means that the position of the beam on the mirrors has also changed. This could create problems in the data analysis if the surface structure reported in [15] was very pronounced on our mirrors. For this reason the θ_{WP} range was limited to minimize the unavoidable cavity adjustment. For any new θ_{WP} we measured the finesse of the cavity, finding values whose spread was compatible with the finesse measurement error.

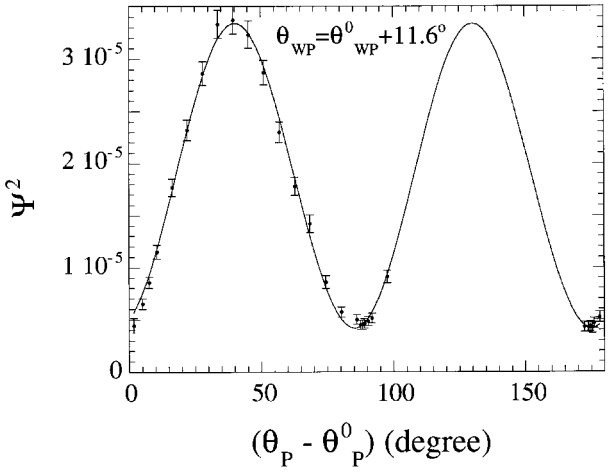

Fig. 4. Typical experimental results for the square ellipticity Ψ^2 as a function of the polarization angle θ_P, obtained for mirror pair I with $\theta_{WP} = \theta^0_{WP} + 11.6°$. The superimposed curve is obtained by best fitting these data with the theoretical expression (10)

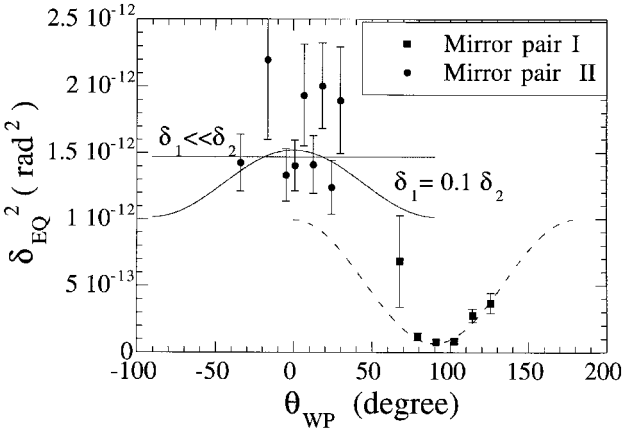

Fig. 5. Experimental data points for the function $\delta_{EQ}(\theta_{WP})$ for both mirror pairs. For mirror pair I the result of the fit using expression (6), giving the values of Table 1, is also shown. For mirror pair II we plot the curves corresponding to the values $\delta_1 = 0$, $\delta_2 = 1.2 \times 10^{-6}$ and $\delta_2 = 1.1 \times 10^{-6}$, $\delta_1 = 0.1\delta_2$

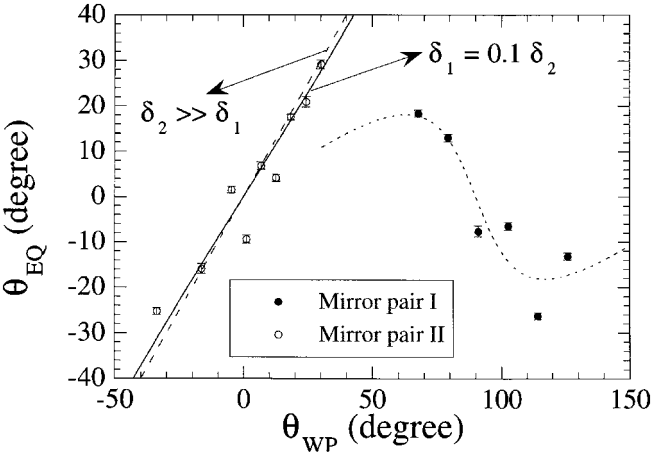

Fig. 6. Experimental data points for the function $\theta_{EQ}(\theta_{WP})$ for both mirror pairs. For mirror pair I the result of the fit using expression (7), giving the values of Table 1, is also shown. For mirror pair II we plot the curves corresponding to the values $\delta_1 = 0$, $\delta_2 = 1.2 \times 10^{-6}$ and $\delta_2 = 1.1 \times 10^{-6}$, $\delta_1 = 0.1\delta_2$

In Fig. 4 we show the experimental data obtained for $\theta_{WP} = \theta^0_{WP} + 11.6°$ for mirror pair I superimposed with the curve obtained by best fitting of these data with the theoretical expression (10). From this best fit one obtains a phase anisotropy δ of about 11 mrad corresponding to $\delta_{EQ} = 2.7 \times 10^{-7}$ rad.

In Figs. 5 and 6 are shown the experimental curves $\delta_{EQ}(\theta_{WP})$ and $\theta_{EQ}(\theta_{WP})$ for the two mirror pairs. To obtain the values of the phase anisotropies δ_1 and δ_2 for mirror pair I we performed two independent best fits. From the data of Fig. 5, using the theoretical expression (6), we obtained some preliminary values for δ_1 and δ_2; from the data of Fig. 6, using for the best fit the theoretical expression (7), we obtained a value for the ratio δ_1/δ_2 in agreement with the previous results for δ_1 and δ_2. These results are reported in Table 1 and the corresponding theoretical curves are shown in Figs. 5 and 6.

For mirror pair II it is clear from the data in Fig. 6 and a comparison with the theoretical curves shown in Fig. 3, that $\delta_1 \ll \delta_2$. This is also in agreement with data from Fig. 5. By comparison of the experimental data with the theoretical curves we found the allowed range for the values of $\delta_1 \ll \delta_2$ and δ_2. Table 1 shows these results, the corresponding theoretical curves are plotted in Figs. 5 and 6.

The values obtained for the phase anisotropy per reflection are of the order of 10^{-6} rad, in agreement with data

Table 1. Results coming from the fit for the phase anisotropies of the two mirror pairs. The phase anisotropies per reflection is twice the value of the parameters δ_i of the table

	Mirror pair I	Mirror pair II
CM_1	$\delta_1 = (6.3 \pm 0.3) \times 10^{-7}$	$\delta_1/\delta_2 < 0.1$
CM_2	$\delta_2 = (3.7 \pm 0.2) \times 10^{-7}$	$1.1 \times 10^{-6} < \delta_2 < 1.2 \times 10^{-6}$

reported in [17, 18]. It is possible, however, to select mirrors with a phase anisotropy per reflection less than 2×10^{-7} rad, as we measured for the CM_1 of the mirror pair II. This is, as far as we know, the smallest value ever reported for the phase anisotropy per reflection of the coating of a high-reflectivity interferential mirror.

Acknowledgements. We wish to thank all our colleagues of the PVLAS collaboration, in particular Prof. E. Polacco and Prof. E. Zavattini for their suggestions and criticisms.

References

1. M. Born, E. Wolf: *Principle of Optics* (Pergamon, Oxford 1980)
2. D.I. Robertson, E. Morrison, J. Hough, S. Killbourn, B.J. Meers, G.P. Newton, N.A. Robertson, K.A. Strain, H. Ward: Rev. Sci. Instrum. **66**, 4447 (1995)
3. A. Abramovici, W. Althouse, J. Camp, D. Durance, J.A. Giaime, A. Gillespie, S. Kawamura, A. Kuhnert, T. Lyons, F.J. Raab, R.L. Savage Jr., D. Shoemaker, L. Sievers, R. Spero, R. Vogt, R. Weiss, S. Whitcomb, M. Zucker: Phys. Lett. A **218**, 157 (1996)
4. J.P. Richard: Phys. Rev. D **46**, 2309 (1992)
5. J.L. Hall: In *Proceedings of the International School of Physics "Enrico Fermi", Frontiers in Laser Spectroscopy, Varenna 1992* ed. by T.W. Haensch, M. Inguscio (North-Holland, Amsterdam 1994), p. 217
6. H.R. Bilger, G.E. Stedman, P.V. Wells: Opt. Commun. **80**, 133 (1990)
7. M. Bouchiat, C. Bouchiat: C. R. Acad. Sci. Paris **322**, **IIb**, 381 (1996)
8. D. Bakalov, G. Cantatore, G. Carugno, S. Carusotto, P. Favaron, F. Della Valle, I. Gabrielli, U. Gastaldi, E. Iacopini, P. Micossi, E. Milotti, R. Onofrio, R. Pengo, F. Perrone, G. Petrucci, E. Polacco, C. Rizzo, G. Ruoso, E. Zavattini, G. Zavattini: Nucl. Phys. B (Proc. Suppl.) **35**, 180 (1994)
9. W.T. Ni: Ch. J. Phys. **34**, 962 (1996)
10. S.A. Lee, W.M. Fairbank Jr., W.H. Toki, J.L. Hall, T.S. Jaffery, P. Colestock, V. Cupps, H. Kautzky, M. Kuchnir, F. Nezrick: Measurement of the Magnetically-Induced QED Birefringence of the Vacuum, An Improved Laboratory Search for Axions, proposal submitted to Fermi National Accelerator Laboratory (March 28, 1995)
11. C. Rizzo, A. Rizzo, D.M. Bishop: Int. Rev. Phys. Chem: **16**, 81 (1997)
12. T.C.P. Chui, M. Shao, D. Redding, Y. Gursel, A. Boden: Mod. Phys. Lett, A **10**, 2125 (1995)
13. M.A. Bouchiat, L. Pottier: Appl. Phys. B **29**, 43 (1982)
14. S. Carusotto, E. Polacco, E. Iacopini, G. Stefanini, E. Zavattini, F. Scuri: Appl. Phys. B **48**, 231(1989)
15. P. Micossi, F. Della Valle, E. Milotti, E. Zavattini, C. Rizzo, G. Ruoso: Appl. Phys. B **57**, 95 (1993)
16. D. Jacob, F. Bretenaker, P. Pourcelot, P. Rio, M. Dumont, A. Doré: Appl. Opt. **33**, 3175 (1994)
17. C. Wood, S.C. Bennett, J.L. Roberts, D. Cho, C.E. Wieman: *Optics and photonics News* October 1996, 54 (1996)
18. D. Jacob, M. Vallet, F. Bretenaker, A. Le Floch, M. Oger: Opt. Lett. **20**, 671 (1995)
19. R.V. Pound: Rev. Sci. Instrum. **17**, 490 (1946);
R.W.P. Drever, J.L. Hall, F.B. Kowalsky, J. Hough, G.M. Ford, A.J. Munley, H. Ward: Appl. Phys. B **31**, 97 (1983)
20. A.M. De Riva, G. Zavattini, S. Marigo, C. Rizzo, G. Ruoso, G. Carugno, R. Onofrio, S. Carusotto, M. Papa, F. Perrone, E. Polacco, G. Cantatore, F. Della Valle, P. Micossi, E. Milotti, P. Pace, E. Zavattini: Rev. Sci. Instrum. **67**, 2680 (1996)
21. E. Hecht, A. Zajac: *Optics* (Addison-Wesley, Reading, MA 1987)